THE JOURNAL OF BIOLOGICAL CHEMISTRY
Vol. 279, No. 11, Issue of March 12, pp. 10142–10147, 2004

Printed in U.S.A.

Functional Dissection of the Transmembrane Domains of the Transporter Associated with Antigen Processing (TAP)*

Received for publication, November 24, 2003, and in revised form, December 12, 2003
Published, JBC Papers in Press, December 15, 2003, DOI 10.1074/jbc.M312816200

Joachim Koch, Renate Guntrum, Susanne Heintke, Christoph Kyritsis, and Robert Tampé‡

From the Institute of Biochemistry, Biocenter, Johann Wolfgang Goethe-University Frankfurt, Marie-Curie Strasse 9, D-69439 Frankfurt, Germany

The transporter associated with antigen processing (TAP1/2) translocates cytosolic peptides of proteasomal degradation into the endoplasmic reticulum (ER) lumen. A peptide-loading complex of tapasin, major histocompatibility complex class I, and several auxiliary factors is assembled at the transporter to optimize antigen display to cytotoxic T-lymphocytes at the cell surface. The heterodimeric TAP complex has unique N-terminal domains in addition to a 6 + 6-transmembrane segment core common to most ABC transporters. Here we provide direct evidence that this core TAP complex is sufficient for (i) ER targeting, (ii) heterodimeric assembly within the ER membrane, (iii) peptide binding, (iv) peptide transport, and (v) specific inhibition by the herpes simplex virus protein ICP47 and the human cytomegalovirus protein US6. We show for the first time that the translocation pore of the transporter is composed of the predicted TM-(5–10) of TAP1 and TM-(4–9) of TAP2. Moreover, we demonstrate that the N-terminal domains of TAP1 and TAP2 are essential for recruitment of tapasin, consequently mediating assembly of the macromolecular peptide-loading complex.

The antigen processing machinery is an important regulatory element in the cellular immune response of vertebrates. A major task is to identify infected or malignantly transformed cells. Therefore, peptides derived from proteasomal degradation of intracellular proteins are translocated via the transporter associated with antigen processing (TAP)[1] into the ER and loaded onto MHC class I molecules. Presentation of "nonself" peptides at the cell surface to CD8+ cytotoxic T-lymphocytes triggers elimination of the transformed cell (1). A macromolecular peptide-loading complex composed of TAP1, TAP2, tapasin, MHC class I molecules, and several auxiliary factors (*e.g.* calreticulin and ERp57) promotes peptide loading onto MHC molecules.

Tapasin is a type I membrane glycoprotein (48 kDa) with a single transmembrane segment (TM) and a short C-terminal cytoplasmic tail (2, 3). Cells lacking tapasin display only few MHC class I molecules on their cell surface (4). The C-terminal 33 amino acids of tapasin are important for binding to TAP, suggesting that tapasin binding is mediated mainly by interaction between TM segments (5, 6). The interaction site for MHC class I molecules is located in the ER luminal domain of tapasin (7, 8). Different functions have been assigned to tapasin as follows: (i) stabilization of the TAP complex (5, 6, 9–12); (ii) anchoring of empty MHC class I molecules at TAP (2, 3, 13, 14); and (iii) coordination and modulation of peptide loading onto MHC class I molecules (15–17).

Human TAP, a member of the ATP-binding cassette (ABC) protein superfamily, forms a heterodimer of TAP1 (748 amino acids) and TAP2 (686 amino acids). Each of the subunits consists of a hydrophobic transmembrane domain (TMD) and a hydrophilic, highly conserved cytoplasmic nucleotide-binding domain (NBD), which couples the chemical energy of ATP hydrolysis to translocation of peptides across the ER membrane. Based on hydrophobicity analysis and sequence alignments with members of the ABC-B subfamily, 10 and 9 TMs have been predicted for human TAP1 and TAP2, respectively (18).

Although conserved among TAP from other vertebrates, the first 175 amino acids of TAP1 and 140 amino acids of TAP2 show no sequence homology to other proteins (19). The role of these unique N-terminal domains in TAP transport function has not been elucidated yet. However, they might be important for the following: (i) independent ER targeting of TAP1 and TAP2; (ii) assembly and stabilization of the heterodimeric TAP complex; (iii) peptide binding and transport; (iv) assembly of the macromolecular peptide-loading complex at TAP; and (v) interaction with viral inhibitors. Viruses have developed sophisticated strategies to interfere with the antigen processing machinery (20). The immediate early protein ICP47 of herpes simplex virus, type 1, binds to TAP from the cytosol and prevents peptide binding to TAP (21, 22). Another prominent example is the human cytomegalovirus protein US6 that binds to TAP from the ER lumen (23–25). The ER-luminal domain of US6 inhibits peptide translocation by specifically blocking ATP binding to TAP (26, 27).

In this study, we examined the role of the N-terminal regions of TAP1 and TAP2. Our results demonstrate for the first time that a 6 + 6-TM core domain is sufficient for assembly of a functional TAP transporter, which can be specifically blocked by viral proteins. Strikingly, the N-terminal domains are found to be essential for recruitment of tapasin, the central component of the peptide-loading complex.

EXPERIMENTAL PROCEDURES

Cloning and Expression of TAP Constructs and Tapasin—To generate human TAP1-(Δ2–132) (mini7, 7 TMs remaining), TAP1-(Δ2–166) (mini6, 6 TMs remaining), TAP2-(Δ2–89) (mini7), and TAP2-(Δ2–122) (mini6), the vectors p46TAP1wt and p46TAP2wt (28) were used in PCRs with the primers 5′-CAGCTCGAGATGTGGGGAAGTCACCCTACCGCCTTCG-3′ and 5′-CTGCTCGAGTCATTCTGGAGCATCT-

* This work was supported by Deutsche Forschungsgemeinschaft Grant SFB 628-Functional Membrane Proteomics. The costs of publication of this article were defrayed in part by the payment of page charges. This article must therefore be hereby marked "*advertisement*" in accordance with 18 U.S.C. Section 1734 solely to indicate this fact.

‡ To whom correspondence should be addressed. Tel.: 49-69-798-29475; Fax: 49-69-798-29495; E-mail: tampe@em.uni-frankfurt.de.

[1] The abbreviations used are: TAP, transporter associated with antigen processing; ABC, ATP-binding cassette; ICP, infected cell protein; MHC, major histocompatibility complex; m.o.i., multiplicity of infection; NBD, nucleotide-binding domain; TM, transmembrane segment; TMD, transmembrane domain; wt, wild type; ER, endoplasmic reticulum; mAb, monoclonal antibody.

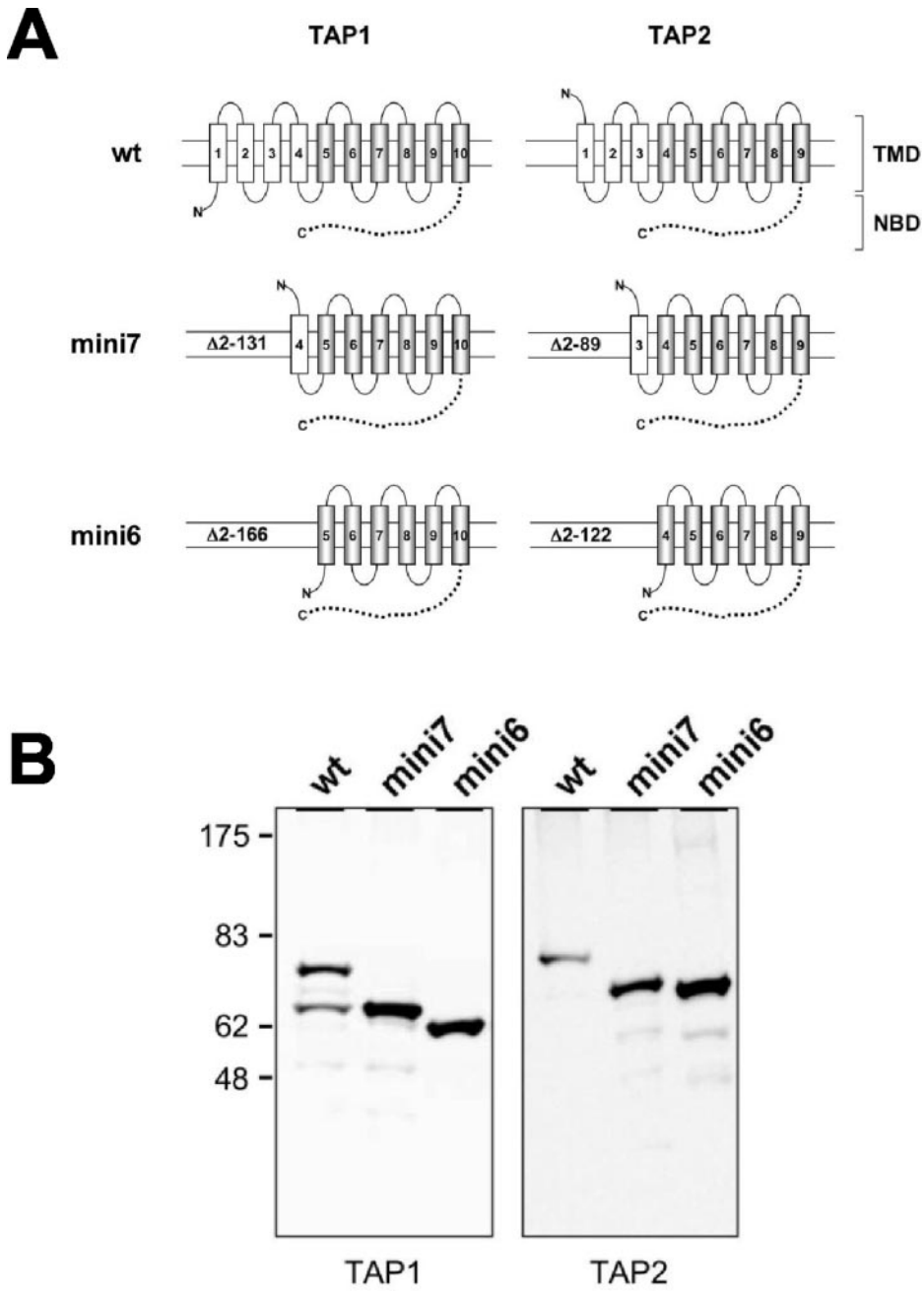

FIG. 1. **Expression of N-terminally truncated TAP complexes.** *A*, schematic representation of the transmembrane domains (*TMDs*) of the constructs. The transmembrane segments of the N-terminal extensions of TAP1 and TAP2 are shown as *open boxes* and those of the core domain of TAP as *shaded boxes*. The nucleotide-binding domains (*NBDs*) are indicated as *dotted lines*. *B*, expression of the TAP constructs (wt TAP, mini7TAP, and mini6TAP). Lysates of baculovirus-infected insect cells (Sf9) were analyzed by SDS-PAGE and subsequent immunoblotting using TAP1- and TAP2-specific antibodies. Cell equivalents were loaded onto the gel.

GCAGGAGCC-3′, 5′-CAGGCGGCCGCATGCCCCCAGCCAGAGTCG-CTTCAGCC-3′ and 5′-CTGGCGGCCGCTCAGAGCTGGGCAAGCTT CTGC-3′ for mini7TAP and 5′-CAGCTCGAGATGGGCGCCTCTGGAA-ACCCTGTGCGT-3′ and 5′-CTGCTCGAGTCATTCTGGAGCATCTGC-AGGAGCC-3′, 5′-ATCTGCTGCAGCCCACAGCTC-3′ and 5′-CAGGCG-GCCGCATGGGAGCCCAGGAGAAGGAGCAGGAC-3′ for mini6TAP. PCR fragments were cloned into the expression vector pFastBac™ Dual (Invitrogen). Human tapasin with a C-terminal Strep® tag was generated by PCR using the primers 5′-AGGA GGTCGCGGATCCAT-GAAGTCCCTGTCTCTGCTC-3′, 5′-TGAGTGCCCAAGCTTTCATCCT-CCGAATTGTGGGTGTCGCCATGACTCTGCTTTCTTCTTTGAATC-3′ and the vector pCR2.1-wt tapasin (2) as template. The PCR product was cloned into the baculovirus expression vector pFastBac™1 (Invitrogen). Recombinant baculoviruses were generated using the Bac-to-Bac® Baculovirus Expression System (Invitrogen). Cloning and expression of the wt TAP1 and TAP2 constructs were performed as described (29).

Cell Culture and Microsome Preparation—Insect cells (*Spodoptera frugiperda* (Sf9)) were grown in Sf900II medium (Invitrogen) following standard procedures. Infection with recombinant baculovirus and preparation of microsomes were performed as described (29). For single infections a multiplicity of infection (m.o.i.) of 3, for co-infections a m.o.i. of 3 for the TAP constructs, and an m.o.i. of 30 for tapasin were used. The TAP content in microsome preparations was determined by SDS-PAGE and immunoblotting using TAP1- (mAb 148.3) and TAP2 (mAb 435.3)-specific antibodies (29, 30). Relative amounts of TAP1 and TAP2 were quantified after luminescence imaging (Lumi-Imager F1™, Roche Applied Science).

Peptide Binding—Microsomes (50 μg of total protein) were mixed with different concentrations (10, 50, 100, 500, 1000, and 2000 nM) of radiolabeled peptide (RRYQKSTEL) in the absence and presence of a 400-fold molar excess of non-labeled peptide in 50 μl of AP buffer (5 mM $MgCl_2$ in phosphate-buffered saline, pH 7.0) and incubated for 15 min on ice. Non-bound peptides were removed by washing the microsomes with 200 μl of AP buffer using a vacuum manifold. The amount of radioactivity bound to the microsomes was quantified by γ-counting and corrected for the signal obtained in the presence of non-labeled peptide. All experiments were performed as triplicates. Radiolabeling of peptides was performed as described (31).

Peptide Transport—Microsomes (50 μg of total protein) were mixed with radiolabeled peptide (1 μM, RRYQNSTEL), ATP (3 mM), or ADP (3 mM) in 50 μl of AP buffer and incubated for 3 min at 32 °C. The reaction was stopped by addition of 500 μl of cold AP buffer supplemented with 10 mM EDTA. After centrifugation, the microsomes were solubilized in 1 ml of lysis buffer (20 mM Tris/HCl, 150 mM NaCl, 5 mM $MgCl_2$, 1% (v/v)

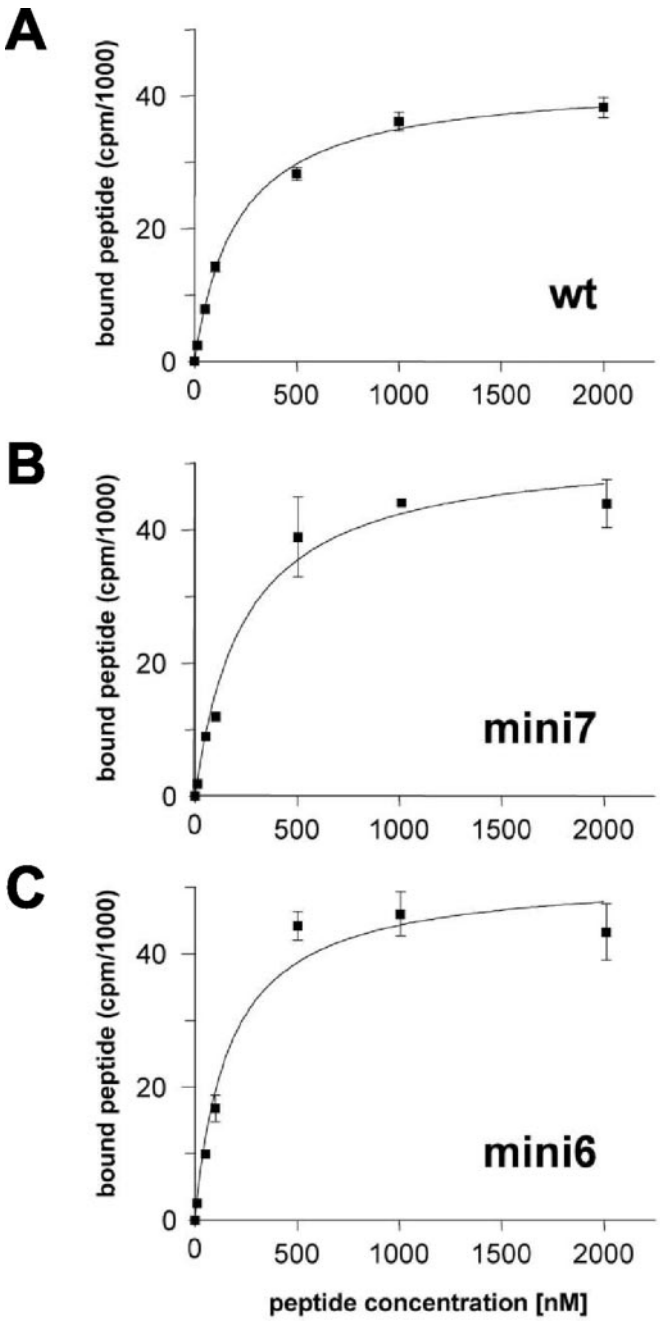

FIG. 2. **Peptide binding to the core TAP complex.** Peptide binding to the TAP complex. After addition of radiolabeled peptide (RRYQKSTEL) and subsequent washing, bound peptides were quantified by γ-counting. The peptide binding curves were fitted to a 1:1 Langmuir binding model. The peptide dissociation constants K_D were 213 ± 21 nM for wt TAP (*A*), 240 ± 56 nM for mini7TAP (*B*), and 170 ± 47 nM for mini6TAP (*C*). For peptide binding, equal amounts of TAP were used in triplicate experiments.

Nonidet P-40, pH 7.5) and incubated on ice for 15 min. Insoluble debris was removed by centrifugation. Glycosylated peptides were bound to 60 μl of concanavalin A-Sepharose (50% (v/v)) for 16 h at 4 °C. After washing three times with 1 ml of lysis buffer, radioactivity associated with the concanavalin A beads was quantified by γ-counting. For TAP-specific inhibition, the active domain of ICP47-(3–34) was used as described previously (32). All experiments were performed as triplicates.

Immunoprecipitation—50 μl of microsomes (250 μg of total protein) were solubilized in 50 μl of lysis buffer (20 mM Tris/HCl, 150 mM NaCl, 5 mM $MgCl_2$, 2% (w/v) digitonin (Calbiochem), pH 7.5) for 30 min on ice. Insoluble material was removed at 100,000 × *g*, and the supernatant was incubated for 90 min at 4 °C with 100 μl of mAb 148.3 hybridoma supernatant. 60 μl of protein A-Sepharose (50% slurry) in lysis buffer was added and incubated for 90 min at 4 °C. The beads were washed three times with 1 ml of washing buffer (10 mM Tris/HCl, 150 mM NaCl, 2 mM EDTA, 0.1% (w/v) digitonin, pH 7.5). Proteins were eluted in sample buffer (10 min at 65 °C) and analyzed by SDS-PAGE and immunoblotting using a tapasin-specific monoclonal antibody (rat mAb 1E2) or a TAP1-specific polyclonal antibody.

ATP-Agarose Binding Assays—The ATP binding activity of TAP was analyzed based on published procedures (33). The inhibitory effect of US6 on TAP was analyzed as described previously (26). In brief, His-tagged US6-(Δ147–183) was heterologously expressed in *Escherichia coli*, purified by immobilized metal affinity chromatography from inclusion bodies, and refolded as described previously (26). Digitonin-solubilized TAP was incubated with ATP-agarose in the presence and absence of US6. Bound protein was eluted with MgATP (10 mM) and analyzed by SDS-PAGE and immunoblotting using the TAP1-specific monoclonal antibody 148.3. To analyze tapasin binding to TAP, 200 μl of microsomes (1 mg of total protein) were solubilized in 200 μl of solubilization buffer (20 mM HEPES, 150 mM NaCl, 1 mM KCl, 1.5 mM $MgCl_2$, 0.75 mM $MnCl_2$, 15% (v/v) glycerol, 1 mM dithiothreitol, 2% (w/v) digitonin, pH 7.4) for 15 min at 4 °C. Insoluble material was removed at 100,000 × *g* for 30 min at 4 °C. 20 mg of ATP-agarose in 1 ml of solubilization buffer were added and incubated for 1 h at 4 °C. The ATP-agarose beads were washed three times with 1 ml of washing buffer (solubilization buffer containing 0.2% (w/v) digitonin). Proteins were eluted in 200 μl of washing buffer containing 10 mM MgATP for 5 min on ice and analyzed by SDS-PAGE and immunoblotting.

RESULTS

Each TMD of the transporter subunits TAP1 and TAP2 can be subdivided into a core domain of six predicted TMs (conserved architecture of the ABC-B family) and an N-terminal region of four or three TMs (19). To investigate the function of these N-terminal domains, we generated truncation variants with seven (mini7TAP; TAP1-(Δ2–132), TAP2-(Δ2–89)) and six remaining TMs (mini6TAP; TAP1-(Δ2–166), TAP2-(Δ2–122)) within TAP1 and TAP2. Mini6TAP corresponds to a 6 + 6-TM core complex (Fig. 1*A*). The TAP constructs were expressed in Sf9 insect cells as shown by SDS-PAGE and subsequent immunoblotting with antibodies specific for TAP1 or TAP2 (Fig. 1*B*). Mini7TAP1 displays the same electrophoretic mobility as a degradation product observed for wt TAP1 (65 kDa).

To analyze peptide recognition of all TAP constructs, saturation binding experiments were performed with isolated microsomes and radiolabeled peptide (RRYQKSTEL). All TAP constructs had similar peptide binding constants as wt TAP (wt TAP, K_D = 213 ± 21 nM; mini7TAP, 240 ± 56 nM; mini6TAP, 170 ± 47 nM), demonstrating that the peptide-binding pocket was fully maintained in the 6 + 6-TM core complex (Fig. 2). In addition, real time binding kinetics with fluorescein-labeled peptides showed that peptide association and dissociation rates at mini6 and mini7TAP constructs did not differ from wt TAP (data not shown).

We then examined the transport function of the TAP variants by *in vitro* peptide translocation assays with radiolabeled peptide (RRYQNSTEL, single letter code; the *N*-glycosylation targeting sequence is underlined) as described previously (34). ATP-dependent peptide transport activities were found for all TAP constructs (Fig. 3, *A–C*). Because TAP1 or TAP2 alone is non-functional (29, 35), the results demonstrate formation of functional heterodimers. The increased transport activity of mini6TAP can be explained by a higher stability of the core TAP complex (mini6TAP) compared with wt TAP as analyzed by time-dependent loss of the peptide binding capacity of TAP (data not shown). In the presence of the non-labeled high affinity peptide (RRYQKSTEL, 400-fold molar excess), the transport activity of all TAP constructs was reduced to background level. Furthermore, all TAP constructs remained sensitive to inhibition by the TAP-specific viral inhibitor ICP47. In conclusion, the peptide-binding pocket and the overall structure required for peptide transport are preserved in the core TAP complex. We next examined the inhibitory effect of the human

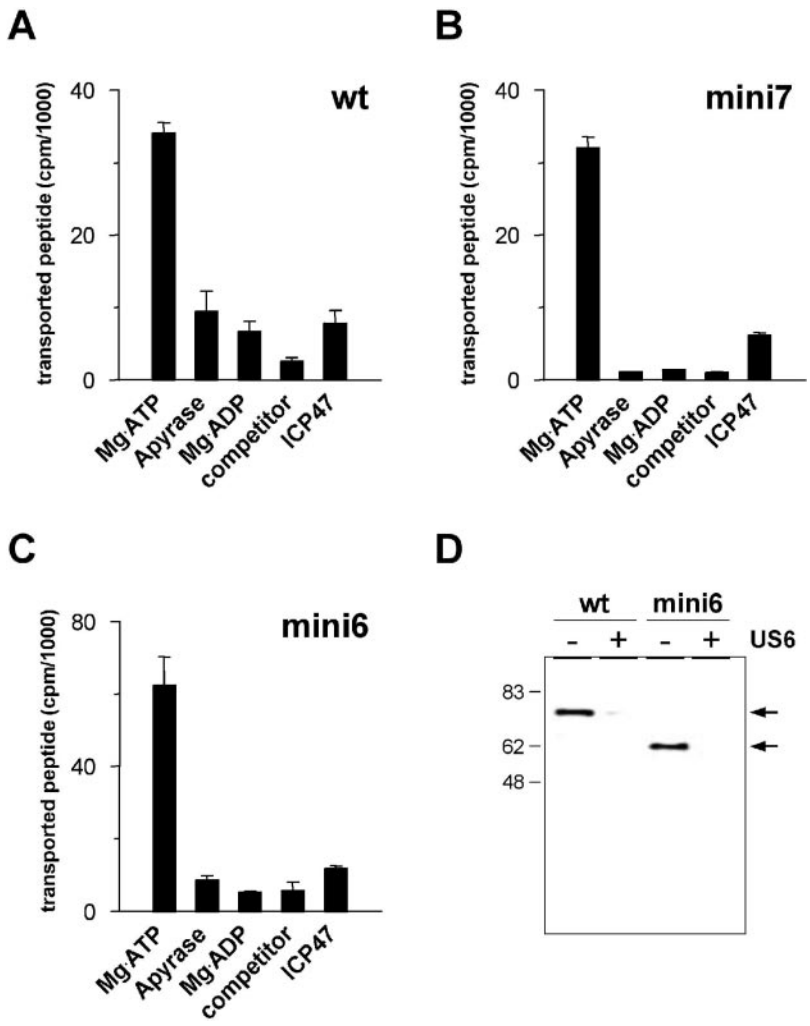

FIG. 3. **Peptide transport and viral inhibition of the core TAP complex.** *A–C*, peptide transport into microsomes. Radiolabeled peptide (RRYQNSTEL) was used as substrate in the presence of ATP (3 mM), apyrase (40 units/ml), ADP (3 mM), non-labeled competitor peptide (RRYQKSTEL, 400-fold molar excess plus 3 mM ATP), or the TAP-specific viral inhibitor ICP47 (250-fold molar excess plus 3 mM ATP). Transported peptides were quantified by γ-counting. For peptide transport equal amounts of TAP were used in triplicate experiments. *D*, digitonin-solubilized TAP (wt TAP or mini-6TAP) was incubated with ATP-agarose in the presence and absence of 20 μM of US6-(Δ147–183). After three washing steps, specifically bound protein was eluted by MgATP (10 mM) and analyzed by SDS-PAGE and immunoblotting with a TAP1-specific antibody.

cytomegaloviral protein US6 on ATP binding of the full-length and the core TAP complex. Interestingly, wild type and mini6TAP have the same nucleotide binding activities as demonstrated by ATP-agarose binding (Fig. 3*D*). However, wt TAP and mini6TAP lost their ability to bind ATP in the presence of US6. Similar results were observed for mini7TAP (data not shown). On the basis of these data we conclude that the N-terminal domains of TAP1 and TAP2 are not essential for US6 binding and specific inhibition of peptide translocation by US6.

Next we investigated the importance of the N-terminal domains of TAP for recruitment of tapasin, a key component of the peptide-loading complex. First, co-expression of tapasin and TAP (wt TAP, mini7TAP, or mini6TAP) in microsomes was confirmed by SDS-PAGE and immunoblotting (Fig. 4*A*). Due to post-translational modification (36), two protein species (46/48 kDa) were detected with the tapasin-specific antibody. In the range of error, co-expression of tapasin and TAP did not affect peptide transport into isolated microsomes (data not shown). Most recently, it was reported that tapasin stabilizes TAP as analyzed by the steady-state expression level of TAP in wild type and tapasin-deficient murine cells (11). However, as shown previously, this effect is compensated by the much stronger expression of TAP in insect cells (12). For interaction studies, TAP was immunoprecipitated from digitonin-solubilized microsomes, and immunocomplexes were analyzed by immunoblotting with tapasin- and TAP1-specific antibodies (Fig. 4*B*). Although the expression level for the TAP variants was even higher than for wt TAP, interaction of tapasin with mini6 and mini7TAP could not be detected. However, full-length TAP showed strong tapasin binding in accordance with published data (2, 3). As a control, tapasin was not immunoprecipitated by a TAP-specific antibody in the absence of TAP.

In an alternative approach, TAP complexes were captured by specific binding to ATP-agarose. Specifically bound proteins were analyzed by SDS-PAGE and immunoblotting (Fig. 4*C*). Mini6, mini7, and wt TAP showed the same ATP binding activity (see above). Again, tapasin was found associated only with wt TAP, but not with mini7 or mini6TAP, demonstrating that the N-terminal domains of TAP1 and TAP2 are essential for tapasin binding. Tapasin alone did not bind to the ATP-agarose beads.

DISCUSSION

As a common architecture, ABC transporters share two transmembrane domains (TMDs) and two nucleotide-binding domains (NBDs), which couple ATP hydrolysis to substrate transport. Most ABC transporters comprise six transmembrane segments (TMs). However, extra N-terminal extensions can be found. For example, the N-terminal domain (TMD_0) of the sulfonylurea receptor, which is associated with persistent hyperinsulinemic hypoglycemia of infancy, recruits the potassium channel subunit $K_{IR}6.2$ (37, 38).

To investigate the role of the N-terminal domains of TAP1 and TAP2, we generated truncation variants, which include predicted seven (mini7TAP) and six (mini6TAP) TMs within TAP1 and TAP2. These constructs were expressed in insect cells, which are well established to analyze TAP function (22, 29–31) and the TAP-tapasin interaction (12, 39, 40). Here we

demonstrate that deletion of the N-terminal regions (2–166 of TAP1 and 2–122 of TAP2) has no detectable effect on peptide transport, and that the predicted 6 + 6-TM core region of TAP is sufficient for correct assembly of the functional heterodimeric transport complex. All constructs were found in microsomal membranes. Furthermore, indirect immunofluorescence with TAP-specific antibodies showed that the cellular localization of all TAP constructs is identical to wt TAP (data not shown).

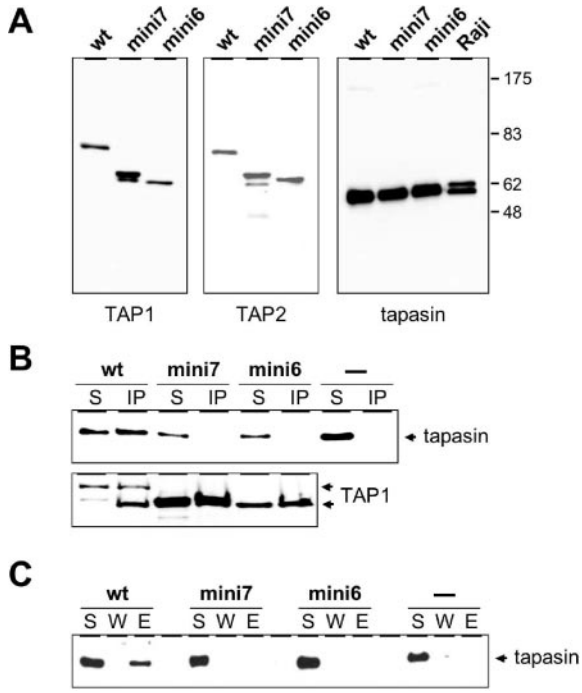

FIG. 4. **Tapasin binding to TAP.** *A*, co-expression of tapasin and TAP (wt TAP, mini7TAP or mini6TAP) in microsomes of insect and Raji cells was analyzed by SDS-PAGE and immunoblotting using TAP1-, TAP2-, and tapasin-specific antibodies. Equivalents of microsomal protein were loaded on the gel. *B*, TAP-tapasin complexes were co-immunoprecipitated from digitonin-solubilized microsomes and analyzed by SDS-PAGE and immunoblotting with a tapasin- (*upper panel*) or a TAP1-specific antibody (*lower panel*). Microsomes expressing tapasin but not TAP were used as control. *S*, solubilized fraction; *IP*, immune precipitate. *C*, after digitonin solubilization, TAP was captured with ATP-agarose. After three washing steps, protein complexes were specifically eluted with MgATP (10 mM) and analyzed by SDS-PAGE and immunoblotting with tapasin-specific antibodies. Equal amounts of wt, mini7, and mini6 TAP were eluted (data not shown). Microsomes expressing tapasin but not TAP were used as control. *S*, solubilized fraction; *W*, wash; *E*, eluted fraction.

Studies with photoreactive peptides showed that both TAP subunits contribute to peptide binding (41). The peptide-binding pocket was localized in the cytosolic loops between predicted TM8 and TM9 of TAP1, TM7 and TM8 of TAP2, and a stretch of 15 amino acids C-terminal of TM10 of TAP1 and TM9 of TAP2 (42, 43). These regions are present in the functional core TAP complex (see Fig. 5).

Previous studies using non-functional reporter fusion constructs of TAP1 and TAP2 indicated eight and seven TMs for TAP1 and TAP2, respectively. On the basis of these fusion constructs, the authors suggested a translocation pore formed by TM-(1–6) of TAP1 and TM-(1–5) of TAP2 (44, 45). In contrast, here we provide direct evidence that the translocation pore is built up by predicted TM-(5–10) of TAP1 and TM-(4–9) of TAP2. This 6 + 6-TM core complex is sufficient for peptide recognition, ATP-dependent peptide transport, and viral inhibition by ICP47 and US6. Because US6 binds to TAP from the ER-luminal side, we propose that the short ER-luminal loops of the core TAP complex mediate docking of US6.

It was shown previously that the TAP complex binds four tapasin molecules and that the ratio of tapasin to MHC class I within the macromolecular peptide-loading complex is about 1:1 (2). The molecular mass of the peptide-loading complex (1xTAP, 4xtapasin, 4xMHC I, 4xERp57, and 4xcalreticulin) can be estimated to 1 MDa. Each TAP subunit can independently bind to the subcomplex composed of tapasin, MHC class I, calreticulin, and ERp57 (35). Moreover, the TMDs of TAP1 and TAP2 are sufficient for tapasin binding (12). Based on these findings, we did not examine combinations of mini and wt TAP. According to our data, we propose that the tapasin-binding sites are located within the N-terminal domains of TAP1 and TAP2 (Fig. 5). However, it remains puzzling how four tapasin-MHC subcomplexes associated with further auxiliary proteins (*e.g.* calreticulin and ERp57) are structurally organized with respect to the two TAP subunits. The predicated TMs in the core complex (TM-(5–10) of TAP1 and TM-(4–9) of TAP2) share some sequence similarity with the TMs of other ABC transporters. Based on biochemical and structural data on P-glycopro-

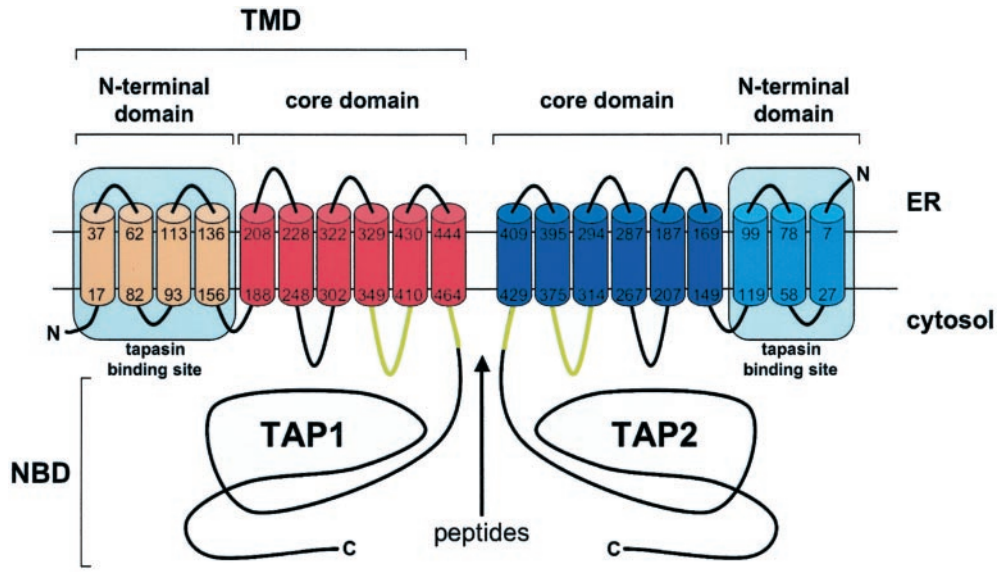

FIG. 5. **Domain organization of the TAP complex.** TAP1 (*red*) and TAP2 (*blue*) are composed of a TMD and an NBD. Each TMD can be subdivided into an N-terminal domain and a 6-TM core region. The N-terminal extensions are essential for tapasin binding, whereas the core TAP complex is sufficient for heterodimer assembly, peptide binding, and transport. The peptide-binding regions are indicated in *green*.

tein and MsbA (46, 47), the N-terminal extensions of TAP1 and TAP2 should point to opposite sites of the core transporter and most likely provide two separate platforms for the assembly of the macromolecular MHC peptide-loading complex.

Acknowledgments—We thank E. Linker for excellent technical assistance and Drs. P. Cresswell (Yale University, New Haven) for pCR2.1-wt tapasin vector, S. Ammer (Biocenter, Frankfurt) for generation of baculovirus encoding for Strep®-tagged human tapasin, E. Kremmer (GSF, Munich) for collaboration in generating the rat mAb 1E2, and C. van der Does and R. Abele (Biocenter, Frankfurt) for helpful discussions and careful reading of the manuscript.

REFERENCES

1. Pamer, E., and Cresswell, P. (1998) *Annu. Rev. Immunol.* **16,** 323–358
2. Ortmann, B., Copeman, J., Lehner, P. J., Sadasivan, B., Herberg, J. A., Grandea, A. G., Riddell, S. R., Tampé, R., Spies, T., Trowsdale, J., and Cresswell, P. (1997) *Science* **277,** 1306–1309
3. Sadasivan, B., Lehner, P. J., Ortmann, B., Spies, T., and Cresswell, P. (1996) *Immunity* **5,** 103–114
4. Grandea, A. G., III, Lehner, P. J., Cresswell, P., and Spies, T. (1997) *Immunogenetics* **46,** 477–483
5. Lehner, P. J., Surman, M. J., and Cresswell, P. (1998) *Immunity* **8,** 221–231
6. Tan, P., Kropshofer, H., Mandelboim, O., Bulbuc, N., Hämmerling, G. J., and Momburg, F. (2002) *J. Immunol.* **168,** 1950–1960
7. Turnquist, H. R., Vargas, S. E., Schenk, E. L., McIlhaney, M. M., Reber, A. J., and Solheim, J. C. (2002) *Immunol. Res.* **25,** 261–269
8. Antoniou, A. N., Powis, S. J., and Elliott, T. (2003) *Curr. Opin. Immunol.* **15,** 75–81
9. Bangia, N., Lehner, P. J., Hughes, E. A., Surman, M., and Cresswell, P. (1999) *Eur. J. Immunol.* **29,** 1858–1870
10. Brocke, P., Garbi, N., Momburg, F., and Hämmerling, G. J. (2002) *Curr. Opin. Immunol.* **14,** 22–29
11. Garbi, N., Tiwari, N., Momburg, F., and Hämmerling, G. J. (2003) *Eur. J. Immunol.* **33,** 264–273
12. Raghuraman, G., Lapinski, P. E., and Raghavan, M. (2002) *J. Biol. Chem.* **277,** 41786–41794
13. Barnden, M. J., Purcell, A. W., Gorman, J. J., and McCluskey, J. (2000) *J. Immunol.* **165,** 322–330
14. Peh, C. A., Laham, N., Burrows, S. R., Zhu, Y., and McCluskey, J. (2000) *J. Immunol.* **164,** 292–299
15. Williams, A. P., Peh, C. A., Purcell, A. W., McCluskey, J., and Elliott, T. (2002) *Immunity* **16,** 509–520
16. Park, B., and Ahn, K. (2003) *J. Biol. Chem.* **278,** 14337–14345
17. Zarling, A. L., Luckey, C. J., Marto, J. A., White, F. M., Brame, C. J., Evans, A. M., Lehner, P. J., Cresswell, P., Shabanowitz, J., Hunt, D. F., and Engelhard, V. H. (2003) *J. Immunol.* **171,** 5287–5295
18. Tampé, R., Urlinger, S., Pawlitschko, K., and Uebel, S. (1997) in *Unusual Secretory Pathways: From Bacteria to Man* (Kuchler, K., Rubartelli, A., and Holland, B., eds) pp. 115–136, Landes Bioscience, Austin, TX
19. Abele, R., and Tampé, R. (1999) *Biochim. Biophys. Acta* **1461,** 405–419
20. Hewitt, E. W. (2003) *Immunology* **110,** 163–169
21. Früh, K., Ahn, K., Djaballah, H., Sempé, P., van Endert, P. M., Tampé, R., Peterson, P. A., and Yang, Y. (1995) *Nature* **375,** 415–418
22. Ahn, K., Meyer, T. H., Uebel, S., Sempé, P., Djaballah, H., Yang, Y., Peterson, P. A., Früh, K., and Tampé, R. (1996) *EMBO J.* **15,** 3247–3255
23. Hengel, H., Koopmann, J. O., Flohr, T., Muranyi, W., Goulmy, E., Hammerling, G. J., Koszinowski, U. H., and Momburg, F. (1997) *Immunity* **6,** 623–632
24. Ahn, K., Gruhler, A., Galocha, B., Jones, T. R., Wiertz, E. J., Ploegh, H. L., Peterson, P. A., Yang, Y., and Früh, K. (1997) *Immunity* **6,** 613–621
25. Lehner, P. J., Karttunen, J. T., Wilkinson, G. W., and Cresswell, P. (1997) *Proc. Natl. Acad. Sci. U. S. A.* **94,** 6904–6909
26. Kyritsis, C., Gorbulev, S., Hutschenreiter, S., Pawlitschko, K., Abele, R., and Tampé, R. (2001) *J. Biol. Chem.* **276,** 48031–48039
27. Hewitt, E. W., Gupta, S. S., and Lehner, P. J. (2001) *EMBO J.* **20,** 387–396
28. Heintke, S., Chen, M., Ritz, U., Lankat-Buttgereit, B., Koch, J., Abele, R., Seliger, B., and Tampé, R. (2003) *FEBS Lett.* **533,** 42–46
29. Meyer, T. H., van Endert, P. M., Uebel, S., Ehring, B., and Tampé, R. (1994) *FEBS Lett.* **351,** 443–447
30. van Endert, P. M., Tampé, R., Meyer, T. H., Tisch, R., Bach, J. F., and McDevitt, H. O. (1994) *Immunity* **1,** 491–500
31. Chen, M., Abele, R., and Tampé, R. (2003) *J. Biol. Chem.* **278,** 29686–29692
32. Neumann, L., Kraas, W., Uebel, S., Jung, G., and Tampé, R. (1997) *J. Mol. Biol.* **272,** 484–492
33. Knittler, M. R., Alberts, P., Deverson, E. V., and Howard, J. C. (1999) *Curr. Biol.* **9,** 999–1008
34. Neefjes, J. J., Momburg, F., and Hämmerling, G. J. (1993) *Science* **261,** 769–771
35. Antoniou, A. N., Ford, S., Pilley, E. S., Blake, N., and Powis, S. J. (2002) *Immunology* **106,** 182–189
36. Turnquist, H. R., Vargas, S. E., Reber, A. J., McIlhaney, M. M., Li, S., Wang, P., Sanderson, S. D., Gubler, B., van Endert, P., and Solheim, J. C. (2001) *J. Immunol.* **167,** 4443–4449
37. Babenko, A. P., and Bryan, J. (2003) *J. Biol. Chem.* **277,** 43997–44004
38. Chan, K. W., Zhang, H., and Logothetis, D. E. (2003) *EMBO J.* **22,** 3833–3843
39. Schoenhals, G. J., Krishna, R. M., Grandea, A. G., III, Spies, T., Peterson, P. A., Yang, Y., and Früh, K. (1999) *EMBO J.* **18,** 743–753
40. Lauvau, G., Gubler, B., Cohen, H., Daniel, S., Caillat-Zucman, S., and van Endert, P. M. (1999) *J. Biol. Chem.* **274,** 31349–31358
41. Androlewicz, M. J., Ortmann, B., van Endert, P. M., Spies, T., and Cresswell, P. (1994) *Proc. Natl. Acad. Sci. U. S. A.* **91,** 12716–12720
42. Nijenhuis, M., and Hämmerling, G. J. (1996) *J. Immunol.* **157,** 5467–5477
43. Nijenhuis, M., Schmitt, S., Armandola, E. A., Obst, R., Brunner, J., and Hämmerling, G. J. (1996) *J. Immunol.* **156,** 2186–2195
44. Vos, J. C., Reits, E. A., Wojcik-Jacobs, E., and Neefjes, J. (2000) *Curr. Biol.* **10,** 1–7
45. Vos, J. C., Spee, P., Momburg, F., and Neefjes, J. (1999) *J. Immunol.* **163,** 6679–6685
46. Chang, G. (2003) *J. Mol. Biol.* **330,** 419–430
47. Loo, T. W., and Clarke, D. M. (2000) *J. Biol. Chem.* **275,** 5253–5256